CHEMISTRY
A EUROPEAN JOURNAL

DOI: 10.1002/chem.201001413

Star-Shaped Oligothiophenes with Unique Photophysical Properties and Nanostructured Polymorphs

Tomoyuki Narita,[a] Masayoshi Takase,[a] Tohru Nishinaga,[a] Masahiko Iyoda,*[a] Kenji Kamada,*[b] and Koji Ohta[b]

Star-shaped molecules with C_6 and C_3 symmetries have attracted considerable attention in the field of materials science because of their divergent and extended π-conjugation.[1,2] In particular, D_{6h}-symmetric hexaethynylbenzenes and related compounds have been used as core structures for dendritic materials,[3] discotic liquid crystals,[4] and functional dyes.[5] Recently, hexaethynylbenzene derivatives have also been employed for constructing supramolecular architectures[6] and reported as potential nonlinear optical materials for two-photon absorption (TPA) and third-order optical nonlinearity.[7,8] Various functionalized hexa(arylethynyl)benzenes have been synthesized by different groups to date,[9a,b] and the derivative **2** of the star-shaped hexaethynylbenzene **1** with terthiophene arms was first reported by Pappenfus and Mann.[10] However, only a limited number of solution properties of **2** have been investigated probably owing to its poor solubility in common organic solvents (Scheme 1).

To improve the solubility and explore new functional properties of hexa(oligothienylethynyl)benzenes, we introduced two butyl groups into the outmost thiophene ring in each terthiophene arm, **3**. With the extra butyl groups, compound **3** is expected to increase its solubility in organic solvents, to decrease its degree of π–π stacking interaction in solution, and to show mesomorphic behavior.[11,12] An improvement in fluorescent yield is also expected for **3** because the overcrowded 24 butyl groups suppress the conformational change of the molecule, which is favorable for a strong emission.[13] Herein, we present the linear and nonlinear optical behavior, and supramolecular properties of **3**, together with those of the tetra-armed (**5**) and tri-armed (**7**) compounds.

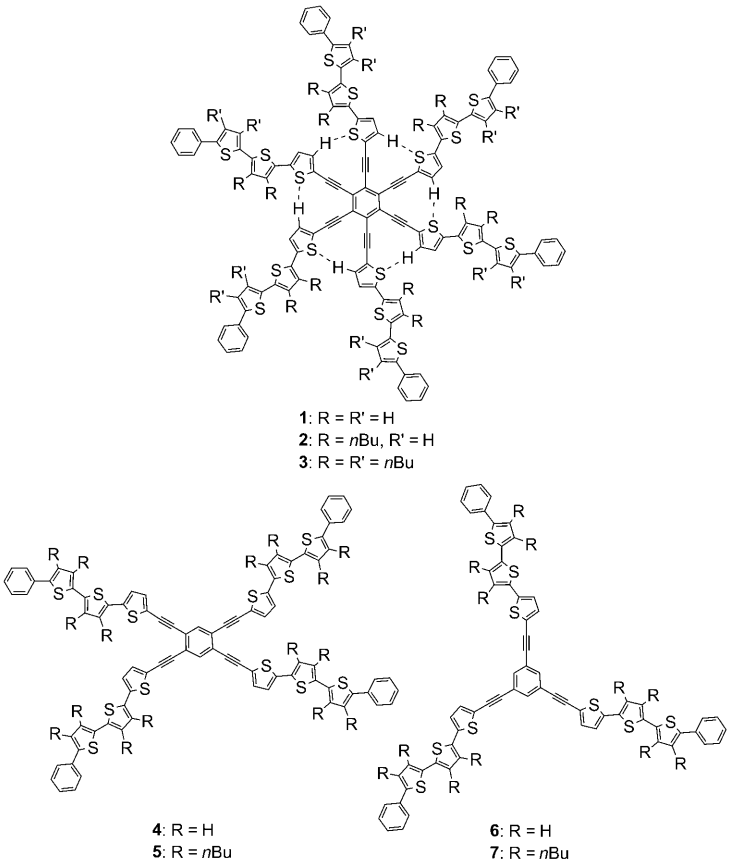

Scheme 1. Star-shaped hexa-, tetra-, and triethynylbenzene derivatives **1**–**7**.

[a] T. Narita, Dr. M. Takase, Prof. T. Nishinaga, Prof. M. Iyoda
Department of Chemistry, Graduate School of Science and Engineering, Tokyo Metropolitan University
Hachioji, Tokyo 192-0397 (Japan)
Fax: (+81) 42-677-2525
E-mail: iyoda@tmu.ac.jp

[b] Dr. K. Kamada, Dr. K. Ohta
Research Institute for Ubiquitous Energy Devices
National Institute of Advanced Industrial Science and Technology (AIST)
AIST Kansai Center, Ikeda, Osaka 563-8577 (Japan)
Fax: (+81) 72-751-9637
E-mail: k.kamada@aist.go.jp

Supporting information for this article is available on the WWW under http://dx.doi.org/10.1002/chem.201001413.

As reported previously,[14] starlike hexaarylbenzene with terthiophene arms decorated with flexible dodecyl chains is a waxy solid at room temperature and its mesophase is less ordered than those of related hexaphenyl- and hexathienylbenzene derivatives. We expected that the disc-like structure of **3** would be supported by the six inter-arm S···H interactions (3.221 Å)[6,15] shown by dotted lines in Scheme 1, and hence the conformation of **3** would be a twisted structure: the calculated average dihedral angle between the central benzene ring and the neighboring thiophene rings in **1** is 12.3° (C_6 symmetry).[15] Because of the lateral van der Waals interaction of alkyl chains together with the weak or medium stacking interaction of the central π-frame, compound **3** may preferably form nanostructures such as fibers and tapes.[6,16] In contrast to that in **3**, the calculated average dihedral angles between the central benzene ring and the neighboring thiophene rings in **4** and **6** are 6.1 and 3.0° (C_2 symmetry) and 0.5° (C_3 symmetry), respectively. Therefore, compound **5** has better planarity than **3**, and **7** has a planar structure, although **5** and **7** may be conformationally labile.

The synthesis of **3**, **5**, and **7** was carried out by two different routes based on the Sonogashira coupling reaction.[6] As shown in Scheme 2, the terthiophene derivatives **13**–**16** were prepared starting from 3,4-dibutyl-2-iodothiophene (**8**). The Sonogashira coupling reactions of the iodoterthiophene **15** with 1,3,5-triethynyl- (**17**), 1,2,4,5-tetraethynyl- (**19**), and hexaethynylbenzene (**21**)[9a,c] produced the corresponding star-shaped molecules **7**, **5**, and **3** in 51, 58, and 63% yields, respectively (Scheme 2, Method A). Similarly, the reactions of the ethynylterthiophene **16** with 1,3,5-triiodo- (**18**) and 1,2,4,5-tetraiodobenzene (**20**) produced **7** and **5** in 76 and 58% yields, respectively (Scheme 2, Method B). However, a similar reaction of **16** with hexabromobenzene (**22**) in the presence of CuI, $PdCl_2(PPh_3)_4$, and Et_3N in THF proceeded slowly, mainly resulting in the oligomerization of **16**.[10,17]

All of the star-shaped molecules **3**, **5**, and **7** are stable reddish–orange, orange–yellow, and yellow waxy solids, respectively. Although **3**, **5**, and **7** show absorption spectra (**3**: λ_{max} (log ε, cyclohexane) = 439 (5.31), 474 sh (5.12) nm; **5**: 394 (5.15), 450 sh (4.96) nm; **7**: 375 (5.06) nm) with a normal small solvent effect of 5–13 nm on their absorption maxima, their emission spectra exhibit a marked solvent dependence. As shown in Figures 1 and 2 and Table 1, the fluorescence of **3** shows solvatochromism with fairly high quantum yields, and the emission spectrum in the polar solvent shows a redshift from 519 to 655 nm.[18] Thus, the colors of emission and λ_{em} values for **3** in hexane, toluene, ether, THF, CH_2Cl_2, and DMF are green (λ_{em} = 519 nm), greenish-yellow (λ_{em} = 532 nm), greenish-yellow (λ_{em} = 549 nm), yellow (λ_{em} = 576 nm), yellowish-orange (λ_{em} = 603 nm), and orange (λ_{em} = 655 nm), respectively. In the case of **5**, the emission spectra show a similar redshift from 494 nm in hexane to 609 nm in DMF, and the colors of **5** in hexane, toluene, ether, THF, CH_2Cl_2, and DMF are green, yellowish-green, yellowish-green, greenish-yellow, yellow, and yellow, respectively. However, the emission spectra of **7** show a small redshift from 472 nm in hexane to 504 nm in DMF, and the color of

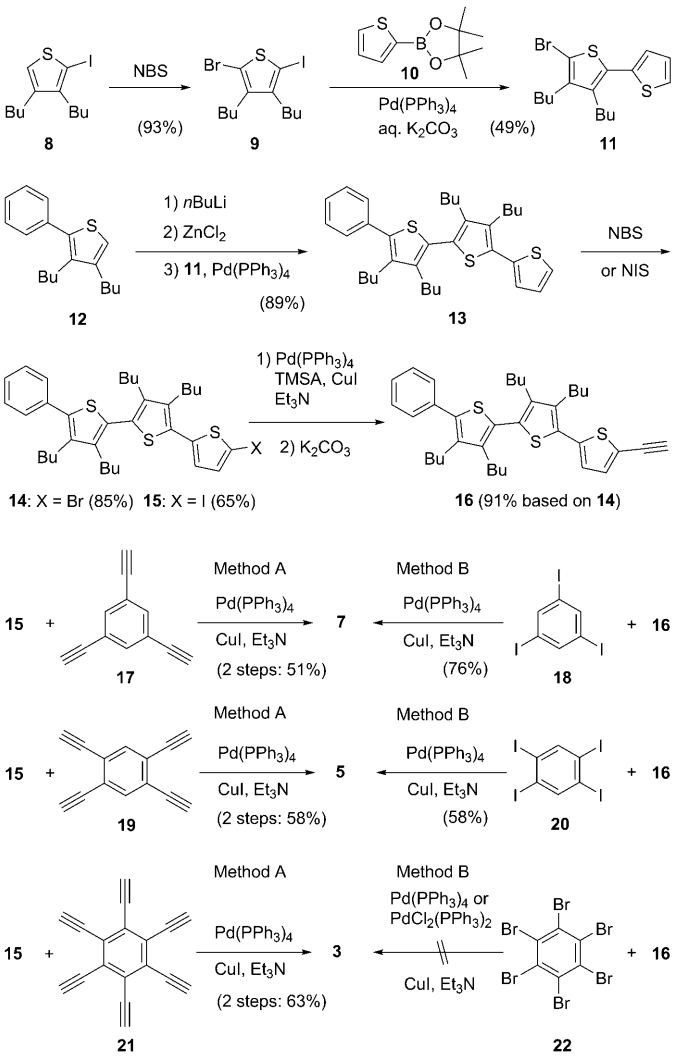

Scheme 2. Synthesis of star-shaped hexa-, tetra-, and triethynylbenzenes **3**, **5**, and **7**. NBS = *N*-bromosuccinimide, NIS = *N*-iodosuccinimide, TMSA = trimethylsilylacetylene.

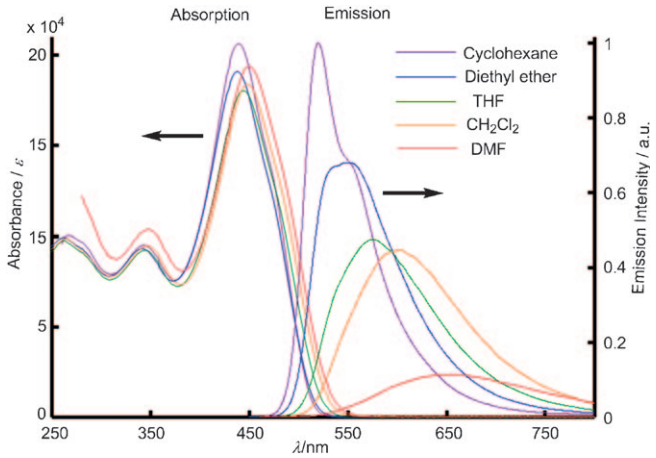

Figure 1. Absorption (left, ε) and emission (right, relative intensity scale) spectra of **3** in cyclohexane, diethyl ether, THF, dichloromethane, and DMF at 23 °C.

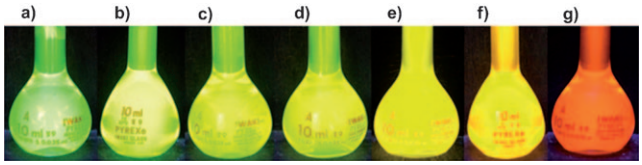

Figure 2. Fluorescent photograph of **3**. Solvent polarity increases in the following order from left to right: a) hexane, b) cyclohexane, c) toluene, d) diethyl ether, e) THF, f) dichloromethane, and g) DMF at 23 °C.

Table 1. Absorption and emission data of **3** in hexane, cyclohexane, diethyl ether, THF, dichloromethane, and DMF.[a]

Solvent	Absorption λ_{max} [nm]	Emission[b] $\varepsilon \times 10^{-5}$	λ_{max} [nm]	Φ_F
hexane	437, 475*	1.85, 1.11	519, 555*	0.42
cyclohexane	439, 475*	2.07, 1.31	519, 555*	0.42
toluene	444, 485*	1.84, 1.05	532	0.46
diethyl ether	438, 485*	1.91, 1.06	549	0.39
THF	444, 485*	1.80, 0.92	576	0.54
CH_2Cl_2	448, 490*	1.84, 1.98	603	0.31
DMF	450, 495*	1.94, 1.07	655	0.14

[a] The absorption and emission spectra of **3** in various solvents (3.25×10^{-6}–5.88×10^{-6} mol L^{-1}) were measured at 23 °C. Shoulder is indicated by an asterisk. [b] Fluorescence quantum yield (Φ_F) was determined by comparison with quinine sulfate in 0.5 M H_2SO_4 ($\Phi_F = 0.51$).

7 varies only from bluish-green to green. The reasonable linear plots for the emission maxima (λ_{em}) of **3**, **5**, and **7** versus the solvent parameter E_T were obtained (see the Supporting Information). Therefore, **3** and **5** possess twisted structures in the ground and excited states,[19] and polar solvents stabilize the polarized excited state.[20] Interestingly, cast films of **3**, **5**, and **7** on glass surfaces exhibit sharp absorption spectra and moderate emission quantum yields similar to the data for the CH_2Cl_2 solution (**3** film: λ_{abs} 450 nm, λ_{em} 587 nm, Φ_F 0.024; **5** film: λ_{abs} 406 nm, λ_{em} 553 nm, Φ_F 0.049; **7** film: λ_{abs} 379 nm, λ_{em} 502 nm, Φ_F 0.031).

To determine the conformational change of the terthiophene arms of **3**, temperature-dependent absorption and emission spectra were measured (Figure 3). The peak at 440 nm of the UV/Vis absorption spectra of **3** in 2-methyltetrahydrofuran (MeTHF) shows a redshift with decreasing temperature ($\lambda_{max} = 442$ nm at 25 °C; 445 nm at 0 °C; 454 nm at −80 °C; 465.5 nm at −196 °C). The shoulder at 480–490 nm also increases and becomes a new peak at −196 °C. The fluorescence band also shows a redshift with decreasing temperature ($\lambda_{em} = 548$ nm at 25 °C; 556 nm at 0 °C; 578 nm at −70 °C); however, it exhibits a significant blueshift with clear substructures ($\lambda_{em} = 476$ and 575 nm) at −196 °C, at which temperature the solution is frozen. The redshift of the absorption and emission at 0 °C and −70 or −80 °C is induced by an increase in coplanarity due to a decrease in conformatonal lability, resulting in an increase of intramolecular through-bond and through-space interactions in **3**, whereas the blueshift of the emission at −196 °C is due to either the depression of vibrational relaxation in the excited state or the inhibition of photoinduced reorientation by the frozen solvent.

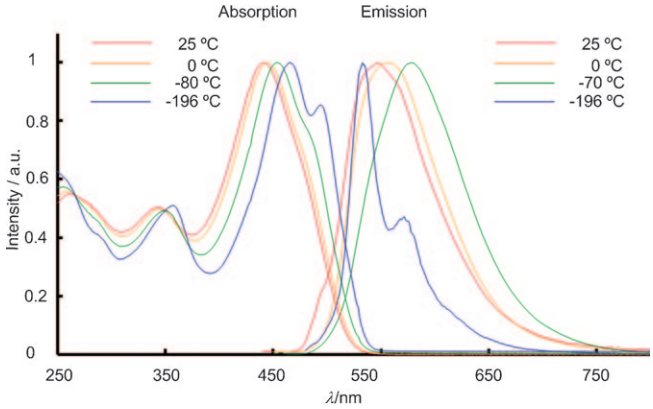

Figure 3. Variable-temperature UV/Vis and fluorescence spectra of **3** in MeTHF. UV/Vis spectrum (5.7×10^{-6} mol L^{-1}) and fluorescence spectrum (2.9×10^{-7} mol L^{-1}).

Unsubstituted hexa(phenylethynyl)benzene was reported previously to exhibit a relatively large TPA cross-section $\sigma^{(2)}$ ($\approx$440 GM at 572 nm), which is enhanced by the introduction of a *tert*-butyl group acting as an electron donor at the *para* position of each peripheral phenyl group ($\sigma^{(2)} \approx 560$ GM at 572 nm).[7a] Since terthiophene groups are strong donors, further enhancement of $\sigma^{(2)}$ can be expected for **3**. We measured the TPA spectrum of **3** in CH_2Cl_2 by the femtosecond open-aperture Z-scan method (Figure 4 and

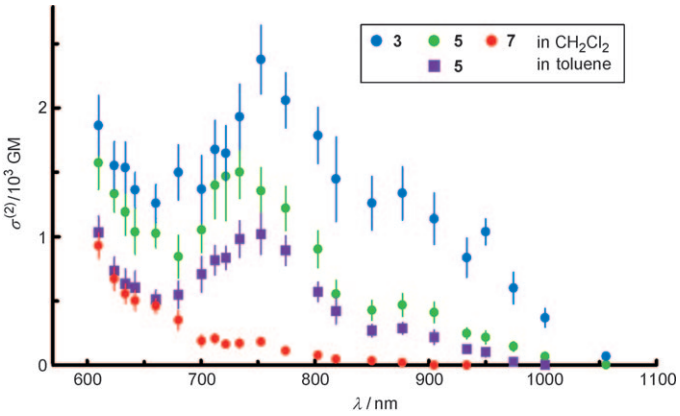

Figure 4. Two-photon absorption cross-section spectra of **3**, **5**, and **7** in CH_2Cl_2 (circles) and of **5** in toluene (squares).

Table 2) and found that **3** has a broad and strong TPA peak at 750 nm ($\sigma^{(2)} = 2400 \pm 270$ GM), which is several times larger than those of the unsubstituted and *tert*-butyl-substituted hexa(phenylethynyl)benzenes, with a significant redshift. The tetra-armed compound **5** has a similar TPA spectrum with a smaller amplitude. Compared with these compounds, the tri-armed compound **7** exhibits a much smaller amplitude. The TPA peak is considered to blue-shift probably beyond the shortest wavelength range observed. These differences in the TPA activity mainly originate from the number of long conjugation paths. The compounds **3** and **5**

Table 2. Absorption coefficients, fluorescence quantum yields, and two-photon absorption cross sections of **3**, **5**, and **7**.

	Absorption[a]		Emission[b]		TPA[c]	
	λ_{max} [nm]	$\varepsilon \times 10^{-5}$	λ_{max} [nm]	Φ_F	λ_{max} [nm]	$\sigma^{(2)}$ [GM]
3[d]	448, 490*	1.84, 1.98	603	0.31	750	2400±270
5[d]	398, 475*	1.27, 0.52	576	0.36	740	1500±200
5[e]	397, 455*	1.15, 0.74	509	0.56	750	1000±150
7[d]	379, 430*[f]	1.47, 0.24	502	0.16	(710)	(200±20)

[a] Shoulder is indicated by an asterisk. [b] Fluorescence quantum yield (Φ_F) was determined by comparison with quinine sulfate in 0.5 M H_2SO_4 ($\Phi_F = 0.51$). [c] TPA cross section ($\sigma^{(2)}$) was measured in CH_2Cl_2 or toluene; 1 GM = 10^{-50} cm^4 s $photon^{-1}$. [d] In CH_2Cl_2. [e] In toluene. [f] Weak shoulder.

have three or two diagonal (terthiophene-ethynylene-phenylene-ethynylene-terthiophene) paths, whereas **7** has no diagonal path. The diagonal paths must contribute to the large TPA peak at the long wavelength. This observation is the same as that observed for hexadehydrotribenzo[12]annulene and its trefoil-shaped trimer.[7a,21]

It is also noted that the amplitude of **7** is still larger than those of the unsubstituted and *tert*-butyl-substituted hexa(phenylethynyl)benzenes, suggesting that terthiophene substitution is very effective for enhancing TPA activity in the wavelength region considered.[22] The strong TPA activities of **3**, **5**, and **7** are considered to arise from the strong charge-transfer (CT) nature of their excited states. This hypothesis is also supported by decrease in the TPA peak intensity of **5** in toluene, which is a less polar solvent than CH_2Cl_2 (Figure 4).

The CV analysis of **3**, **5**, and **7** showed low oxidation potentials with a reversible first oxidation and a quasi-reversible second oxidation, reflecting fairly high HOMOs (Table 3). As for reduction, compounds **3** and **5** showed high reduction potentials with a reversible first reduction and a quasi-reversible second reduction; compound **7** showed no reduction potential. Therefore, compounds **3** and **5** possess fairly low LUMOs. The longest shoulders (λ_{max} (abs.)) together with the $S_0 \rightarrow S_1$ 0–0 transition energies calculated by using the UV/Vis and fluorescence spectra are in good agreement with the HOMO–LUMO gaps estimated from the redox potentials.

Table 3. Redox potentials[a] and HOMO–LUMO gaps[b] of **3**, **5**, and **7**.

Compd	E^{red2} [V][c]	$E^{red1}{}_{1/2}$ [V]	$E^{ox1}{}_{1/2}$ [V]	E^{ox2} [V][d]	$E^{ox1} - E^{red1}$ [V]	HOMO–LUMO [eV]
3	−2.20[d]	−1.80	0.65	0.98[e]	2.49	2.38
5	−2.30[d]	−2.00	0.60	1.00[e]	2.66	2.67
7	–	–	0.58	0.94[e]	–	2.88

[a] Measured by cyclic voltammetry; conditions: 0.1 M Bu_4NPF_6 in THF for reduction and CH_2Cl_2 for oxidation, Ag/Ag^+ reference electrode, glassy carbon working electrode for reduction and Pt working electrode for oxidation, Pt counter electrode, 100 mV s^{-1}; V versus Fc/Fc^+, $Fc/Fc^+ = 0.29$ V referenced to Ag/Ag^+. [b] HOMO–LUMO gaps were estimated from the end absorptions of the UV/Vis spectra in CH_2Cl_2. [c] Peak potential. [d] Irreversible reduction. [e] Irreversible oxidation.

Although the variable-temperature (VT) ^{1}H NMR spectra of **5** and **7** in $CDCl_3$ showed no broadening at low temperatures owing to the conformational flexibility, the VT ^{1}H NMR spectra of **3** exhibited broadening and an upper field shift at low temperatures owing to the self-aggregation of **3** (see the Supporting Information). The conformational flexibility and the existence of more than two conformational isomers for **5** and **7** result in the formation of an amorphous solid after evaporation or attempted crystallization. In contrast, compound **3** forms various fibrous polymorphs in solution, reflecting a C_6-symmetric disc-like structure, whereas **3** forms an amorphous solid after evaporation. As shown in Figure 5, compound **3** forms fibrous materials

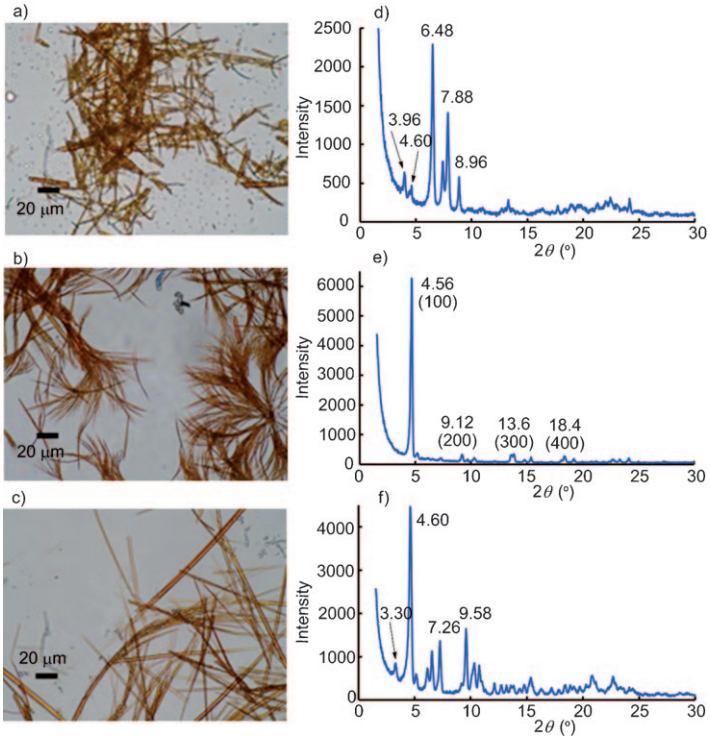

Figure 5. Optical images (a–c) and XRD profiles (d–f) of needles of **3** from hexane (a and d), DMF (b and e), and *i*PrOH (c and f).

from hexane (Figure 5a), DMF (Figure 5b), and isopropyl alcohol (Figure 5c) without incorporating solvents. Although their morphologies seem to be similar, the XRD profiles of these fibers are different (Figure 5d, 5e, and 5f). The fiber of **3** from DMF (Figure 5e) shows a typical profile of a 1D structure, and the strong (100) reflection at $2\theta = 4.56°$ ($d = 19.4$ Å) can be assigned to the molecular size, whereas weak reflections at $2\theta = 9.12$ (200), 13.6 (300), and 18.4° (400) are of higher orders. Since the molecular diameter of **3** is estimated to be 42 Å, the XRD profile shows a laterally ordered lamellar structure ($d = 19.4$ Å) that rises 28° diagonally from the aluminum plate used for the XRD analysis of the fiber. In contrast, the **3** fibers from hexane and *i*PrOH show a complex XRD profile corresponding to a partial crystalline structure (Figure 5d and 5f). All of the

fibers of **3** melt at 127 °C as determined by differential scanning calorimetry (DSC) analysis to produce a supercooled amorphous solid that no longer forms nanostructured polymorphs.

In summary, we have prepared a series of star-shaped oligothiophenes **3**, **5**, and **7** with unique photophysical properties, such as a positive solvatochromism with increasing solvent polarity, and two-photon absorption properties. Furthermore, compound **3** with a central aromatic core and six peripheral oligothiophene arms has an amphiphilic property in organic solvents, resulting in the formation of nanostructures, such as fibrous polymorphs, owing to the lateral van der Waals interaction of alkyl chains together with the stacking interaction of the central π-frame. The moderate to high solubilities and amorphous morphologies of **3**, **5**, and **7** seem to be more appropriate for constructing molecular switches and devices.

Experimental Section

Oligothiophene 3: (Method A) Hexakis(trimethylsilylethynyl)benzene (52 mg, 0.080 mmol) and K_2CO_3 (11 mg, 0.080 mmol) were dissolved in THF (10 mL) and MeOH (10 mL), and the mixture was stirred for 30 min at room temperature. After dilution with Et_2O (60 mL), the organic layer was washed with H_2O three times. The organic layer was dried over $MgSO_4$, and the solution was concentrated by rotary evaporation until the volume became about 15 mL. To the concentrated solution, a solution of **15** (554 mg, 0.820 mmol), $Pd(PPh_3)_4$ (62 mg, 54 mmol), and CuI (23 mg, 0.121 mmol) in THF (20 mL) and Et_3N (2 mL) was added, and the mixture was stirred at room temperature overnight. After adding saturated aqueous NH_4Cl solution, the aqueous layer was extracted three times with CH_2Cl_2. The combined organic layer was dried over $MgSO_4$, and the solvent was evaporated. The crude product was subjected to short column chromatography (SiO_2: hexane/CH_2Cl_2 = 2:1). Further purification by gel permeation chromatography gave **3** as an orange solid (175 mg, 63 %). Formation of this compound was not observed by Method B. Compound **3**: M.p. 127.0 °C (DSC); ^{1}H NMR (400 MHz, $CDCl_3$): δ = 7.50–7.45 (m, 18H), 7.42–7.38 (m, 12H), 7.34–7.31 (m, 6H), 7.14 (d, J = 3.4 Hz, 6H), 2.82–2.76 (m, 12H), 2.65–2.60 (m, 12H), 2.58–2.50 (m, 24H), 1.60–1.24 (m, 96H), 0.94–0.80 ppm (m, 72H); ^{13}C NMR (100 MHz, $CDCl_3$): δ = 143.10, 142.69, 139.89, 139.72, 138.75, 138.06, 138.06, 135.10, 133.49, 130.64, 129.49, 129.32, 128.40, 127.68, 127.27, 125.92, 125.82, 122.04, 93.34, 92.15, 33.08(2C), 32.95, 32.79, 28.10, 27.80, 27.64, 27.24, 22.96, 22.90, 22.80(2C), 13.90, 13.82, 13.78, 13.73 ppm; MS (LDI-TOF) calcd for $C_{222}H_{258}S_{18}$: m/z: 3499.52; found 3499.56; elemental analysis calcd (%) for $C_{222}H_{258}S_{18}$: C 76.10, H 7.42; found: C 75.83, H 7.52.

Oligothiophene 5: (Method A) Compound **5** was prepared in a similar manner to the preparation of **3**, starting from 1,2,4,5-tetrakis(trimethylsilylethynyl)benzene and **15** in 58 % yield. By using Method B, compound **5** was also prepared as an orange-yellow waxy solid in 58 % yield. ^{1}H NMR (400 MHz, $CDCl_3$): δ = 7.75 (s, 2H), 7.49–7.45 (m, 8H), 7.43–7.38 (m, 8H), 7.36–7.30 (m, 8H), 7.09 (d, J = 3.9 Hz, 4H), 2.81–2.75 (m, 8H), 2.66–2.60 (m, 8H), 2.59–2.50 (m, 16H), 1.60–1.43 (m, 40H), 1.35–1.27 (m, 24H), 0.96 (t, J = 7.3 Hz, 12H), 0.89–0.80 ppm (m, 36H); ^{13}C NMR (100 MHz, $CDCl_3$): δ = 143.08, 142.70, 139.81, 139.35, 138.80, 138.08, 135.12, 134.01, 133.11, 130.58, 129.47, 129.34, 128.40, 127.68, 127.28, 125.61, 124.54, 121.94, 92.37, 89.32, 33.07(2C), 32.97, 32.80, 28.10, 27.80, 27.65, 27.24, 23.00, 22.90, 22.80(2C), 13.91, 13.82, 13.78, 13.75 ppm; MS (LDI-TOF) calcd for $C_{150}H_{174}S_{12}$: m/z: 2359.03; found 2359.18; elemental analysis calcd (%) for $C_{150}H_{174}S_{12}$: C 76.28, H 7.43; found: C 76.20, H 7.42.

Oligothiophene 7: (Method A) Compound **7** was prepared in a similar manner to the preparation of **3**, starting from 1,3,5-tris(trimethylsilylethynyl)benzene and **15** in 51 % yield. Method B also afforded **7** as a yellow waxy solid in 76 % yield. ^{1}H NMR (400 MHz, CD_2Cl_2): δ = 7.58 (s, 3H), 7.43–7.40 (m, 6H), 7.38–7.34 (m, 6H), 7.30–7.26 (m, 3H), 7.24 (d, J = 4.0 Hz, 3H), 7.03 (d, J = 4.0 Hz, 3H), 2.75–2.71 (m, 6H), 2.60–2.56 (m, 6H), 2.53–2.48 (m, 12H), 1.57–1.50 (m, 6H), 1.47–1.39 (m, 24H), 1.30–1.23 (m, 18H), 0.93 (t, J = 7.3 Hz, 9H), 0.83–0.78 ppm (m, 27H); ^{13}C NMR (100 MHz, CD_2Cl_2): δ = 143.36, 143.04, 140.16, 139.13, 138.89, 138.40, 135.16, 133.35, 133.16, 130.46, 129.51, 129.37, 128.56, 127.69, 127.46, 125.62, 124.06, 121.87, 92.41, 84.17, 33.17, 33.13, 33.07, 32.92, 28.12, 27.88, 27.74, 27.31, 23.08, 22.98, 22.93, 22.88, 13.78, 13.67, 13.65, 13.62 ppm; MS (LDI-TOF) calcd for $C_{114}H_{132}S_9$: m/z: 1788.78; found 1788.08; elemental analysis calcd (%) for $C_{114}H_{132}S_9$: C 76.46, H 7.43; found: C 76.35, H 7.46.

Acknowledgements

This work was supported in part by a Grant-in-Aid for Scientific Research from the JSPS. We would like to thank Prof. Motoko S. Asano and Hirohisa Yoshida (Tokyo Metropolitan University) for their assistance with VT UV/Vis measurements and VT XRD measurements. We would also like to thank Dr. Eigo Isomura, Takeshi Ohmae, Masaki Tateno, and Dr. Tomohiko Nishiuchi for experimental assistance.

Keywords: fluorescence · nanostructures · nonlinear optics · star-shaped molecules · supramolecular chemistry

[1] a) M. R. Bryce, G. J. Marshallsay, A. J. Moore, *J. Org. Chem.* **1992**, *57*, 4859–4862; b) M. Fourmigué, I. Johannsen, K. Boubekeur, C. Nelson, P. Batail, *J. Am. Chem. Soc.* **1993**, *115*, 3752–3759; c) U. H. F. Bunz, V. Enkelmann, *Organometallics* **1994**, *13*, 3823–3833; d) M. Iyoda, M. Fukuda, M. Yoshida, S. Sasaki, *Chem. Lett.* **1994**, 2369–2372; e) H. Meier, M. Lehmann, *Angew. Chem.* **1998**, *110*, 666–669; *Angew. Chem. Int. Ed.* **1998**, *37*, 643–645; f) A. González, J. L. Segura, N. Martín, *Tetrahedron Lett.* **2000**, *41*, 3083–3086; g) C. A. Christensen, M. R. Bryce, A. S. Batsanov, J. Becher, *Chem. Commun.* **2000**, 331–332; h) B. G. Kim, S. Kim, S. Y. Park, *Tetrahedron Lett.* **2001**, *42*, 2697–2699; i) O. Mongin, J. Brunel, L. Porrès, M. Blanchard-Desce, *Tetrahedron Lett.* **2003**, *44*, 2813–2816; j) J. G. Rodríguez, J. Esquivias, A. Lafuente, C. Díaz, *J. Org. Chem.* **2003**, *68*, 8120–8128; k) H. S. Cho, H. Rhee, J. K. Song, C.-K. Min, M. Takase, N. Aratani, S. Cho, A. Osuka, T. Joo, D. Kim, *J. Am. Chem. Soc.* **2003**, *125*, 5849–5860; l) M. Hasegawa, J. Takano, H. Enozawa, Y. Kuwatani, M. Iyoda, *Tetrahedron Lett.* **2004**, *45*, 4109–4112.

[2] a) F. Jäckel, M. Ai, J. Wu, K. Müllen, J. P. Rabe, *J. Am. Chem. Soc.* **2005**, *127*, 14580–15581; b) L. Zhi, J. Wu, K. Müllen, *Org. Lett.* **2005**, *7*, 5761–5764; c) W.-L. Jia, R.-Y. Wang, D. Song, S. J. Ball, A. B. McLean, S. Wang, *Chem. Eur. J.* **2005**, *11*, 832–842; d) S. Roquet, A. Ctavino, P. Leriche, O. Alévêque, P. Frère, J. Roncali, *J. Am. Chem. Soc.* **2006**, *128*, 3459–3466; e) J. Cremer, P. Bäuerle, *J. Mater. Chem.* **2006**, *16*, 874–884; f) C. N. Likos, *Soft Matter* **2006**, *2*, 478–498; g) D. Cao, S. Dobis, C. Gao, S. Hillmann, H. Meier, *Chem. Eur. J.* **2007**, *13*, 9317–9323; h) H. Detert, M. Lehmann, H. Meier, *Materia* **2010**, *3*, 3218–3330.

[3] a) B. Kayser, J. Altman, W. Beck, *Chem. Eur. J.* **1999**, *5*, 754–758; b) O. Mongin, N. Hoyler, A. Gossauer, *Eur. J. Org. Chem.* **2000**, 1193–1197.

[4] a) K. Praefcke, B. Kohne, D. Singer, *Angew. Chem.* **1990**, *102*, 200–202; *Angew. Chem. Int. Ed. Engl.* **1990**, *29*, 177–179; b) S. Kumar, S. K. Varshney, *Angew. Chem.* **2000**, *112*, 3270–3272; *Angew. Chem. Int. Ed.* **2000**, *39*, 3140–3142; c) P. H. J. Kouwer, W. J. Mijs, W. F. Jager, S. J. Picken, *J. Am. Chem. Soc.* **2001**, *123*, 4645–4646.

[5] a) S. Ito, H. Inabe, N. Morita, K. Ohta, T. Kitamura, K. Imafuku, *J. Am. Chem. Soc.* **2003**, *125*, 1669–1680; b) M. Sonoda, Y. Sakai, T. Yoshimura, Y. Tobe, K. Kamada, *Chem. Lett.* **2004**, *33*, 972–973.

[6] M. Hasegawa, H. Enozawa, Y. Kawabata, M. Iyoda, *J. Am. Chem. Soc.* **2007**, *129*, 3072–3073.

[7] a) K. Kamada, L. Antonov, S. Yamada, K. Ohta, T. Yoshimura, K. Tahara, A. Inaba, M. Sonoda, Y. Tobe, *ChemPhysChem* **2007**, *8*, 2671–2677; b) M.-H. Ha-Thi, V. Souchon, A. Hamdi, R. Métivier, V. Alain, K. Nakatani, P. G. Lacroix, J.-P. Genêt, V. Michelet, I. Leray, *Chem. Eur. J.* **2006**, *12*, 9056–9065.

[8] K. Kondo, S. Yasuda, T. Sakaguchi, M. Miya, *J. Chem. Soc. Chem. Commun.* **1995**, 55–56.

[9] a) M. Sonoda, A. Inabe, K. Itahashi, Y. Tobe, *Org. Lett.* **2001**, *3*, 2419–2421; b) K. Kobayashi, N. Kobayashi, *J. Org. Chem.* **2004**, *69*, 2487–2497; c) R. Diercks, K. P. C. Vollhardt, *J. Am. Chem. Soc.* **1986**, *108*, 3150–3152.

[10] T. M. Pappenfus, K. R. Mann, *Org. Lett.* **2002**, *4*, 3043–3046.

[11] For reviews, see: a) T. F. A. De Greef, M. M. J. Smulders, M. Wolffs, A. P. H. J. Schenning, R. P. Sijbesma, E. W. Meijer, *Chem. Rev.* **2009**, *109*, 5687–5754; b) M. Iyoda, T. Nishinaga, M. Takase, *Top. Heterocycl. Chem.* **2009**, *18*, 103–118; c) M. Iyoda, M. Hasegawa, H. Enozawa, *Chem. Lett.* **2007**, *36*, 1402–1407; d) T. Kato, Y. Hirai, S. Nakaso, M. Moriyama, *Chem. Soc. Rev.* **2007**, *36*, 1857–1867; e) F. J. M. Hoeben, P. Jonkeijm, E. W. Meijer, A. P. H. J. Schenning, *Chem. Rev.* **2005**, *105*, 1491–1546; f) J. A. A. W. Elemans, A. E. Rowan, R. J. M. Nolte, *J. Mater. Chem.* **2003**, *13*, 2661–2670; g) J. S. Moore, *Acc. Chem. Res.* **1997**, *30*, 402–423.

[12] For recent examples, see: a) K. Nakao, M. Nishimura, T. Tamachi, Y. Kuwatani, H. Miyasaka, T. Nishinaga, M. Iyoda, *J. Am. Chem. Soc.* **2006**, *128*, 16740–16747; b) M. J. Rahman, J. Yamakawa, A. Matsumoto, T. Nishinaga, K. Kamada, M. Iyoda, *J. Org. Chem.* **2008**, *73*, 5542–5548; c) M. Iyoda, *C. R. Chim.* **2009**, *12*, 395–402; d) M. Iyoda, *Pure Appl. Chem.* **2010**, *82*, 831–841.

[13] X.-H. Zhou, J.-C. Yan, J. Pei, *Org. Lett.* **2003**, *5*, 3543–3546.

[14] Y. Geng, A. Fechtenkötter, K. Müllen, *J. Mater. Chem.* **2001**, *11*, 1634–1641.

[15] The S···H distance and dihedral angle between the central benzene ring and the neighboring thiophene rings are calculated by RB3LYP/3-21G*. A similar calculation of hexa(phenylethynyl)benzene showed that the dihedral angle between the central and peripheral benzene rings is 25.8° (C_6 symmetry).

[16] For the formation of fibrous materials using the lateral van der Waals interaction of alkyl chains and the stacking interaction of the central π frame, see: a) H. Enozawa, M. Hasegawa, D. Takamatsu, K. Fukui, M. Iyoda, *Org. Lett.* **2006**, *8*, 1917–1920; b) H. Enozawa, M. Hasegawa, E. Isomura, T. Nishinaga, T. Kato, M. Yamato, T. Kimura, M. Iyoda, *ChemPhysChem* **2009**, *10*, 2607–2611; c) Y. Honna, E. Isomura, H. Enozawa, M. Hasegawa, M. Takase, T. Nishinaga, M. Iyoda, *Tetrahedron Lett.* **2010**, *51*, 679–682; d) M. Hasegawa, M. Iyoda, *Chem. Soc. Rev.* **2010**, *39*, 2420–2427.

[17] The Sonogashira reaction of **16** with **22** by using Method B produced a complex mixture containing oligomers of **16** together with imperfectly cross-coupled products, see: J. Nierle, D. Barth, D. Kuck, *Eur. J. Org. Chem.* **2004**, 867–872.

[18] Although many examples of fluorescence solvatochromism for donor–acceptor-substituted heterocycles have been reported, only a limited number of star-shaped benzenoids without a molecular dipole show fluorescence solvatochromism: K. Fujimoto, H. Shimizu, M. Furusyo, S. Akiyama, M. Ishida, U. Furukawa, T. Yokoo, M. Inouye, *Tetrahedron* **2009**, *65*, 9357–9361.

[19] The longest absorption maxima of **3** in CH_2Cl_2, solution and film states, respectively, show 10 nm and 49 nm blueshifts compared with those of **2**, owing to the twisted terthiophene arms in **3**.[10] Similarly, the longest absorption maxima of **5** and **7** in CH_2Cl_2 solution and film states show 19 and 50 nm and 21 and 49 nm blueshifts compared with those of related tetra- and tri-armed compounds (see the Supporting Information).[10]

[20] C. Reichard, *Solvents and Solvent Effects in Organic Chemistry*, 3rd ed., Wiley-VCH, Weinheim, **2003**, pp. 352–359.

[21] A. Bhaskar, R. Guda, M. M. Haley, T. Goodson III, *J. Am. Chem. Soc.* **2006**, *128*, 13972–13973.

[22] For two-photon absorption cross-sections of oligothiophenes, see: a) A. Bhaskar, G. Ramakrishna, K. Hagedorn, O. Varnavski, E. Mena-Osteritz, P. Bäuerle, T. Goodson III, *J. Phys. Chem. B* **2007**, *111*, 946–954; b) G. Ramakrishna, A. Bhaskar, P. Bäuerle, T. Goodson III, *J. Phys. Chem. A* **2008**, *112*, 2018–2026; c) M. Williams-Harry, A. Bhaskar, G. Ramakrishna, T. Goodson III, M. Imamura, A. Mawatari, K. Nakao, H. Enozawa, T. Nishinaga, M. Iyoda, *J. Am. Chem. Soc.* **2008**, *130*, 3252–3253.

Received: May 21, 2010
Published online: September 30, 2010

